Aspiration through hollow cantilever-based nanopipette by means of evaporation

Hector Hugo Perez Garza, Murali Krishna Ghatkesar, Urs Staufer

Micro and Nano Engineering Group, Department of Precision and Microsystems Engineering, Faculty of Mechanical, Maritime and Materials Engineering, Delft University of Technology, Mekelweg 2, 2628 CD Delft, The Netherlands
E-mail: H.H.PerezGarza@tudelft.nl

Published in Micro & Nano Letters; Received on 3rd June 2013; Accepted on 12th August 2013

Presented is a method for aspirating liquids into a hollow atomic force microscope (AFM)-cantilever through a 350 nm-wide nozzle near the tip apex. The cantilever was made of transparent SiO_2 and connected a fluidic reservoir to an evaporation cell. The nanopipette-chip is suitable for mounting the microfluidic system into commercial AFMs. The channel inside the lever spontaneously filled with liquid by capillary forces upon which evaporation started and continuously pumped liquid from the reservoir. The resonance frequency of the cantilever was found to be 153.946 kHz when empty and a frequency shift of 92 Hz was measured when filled. The cantilever's transparency allowed visualisation of the advancing meniscus in real time and confirmed the presence of aspirated, fluorescently labelled liquid. An aspiration rate of ~230 aL/s was measured. This value represents the flow rate in the microfluidic system when operated under ambient conditions (21°C temperature, 43% relative humidity). The estimated volume that has been aspirated in total was ~85.42 aL. The aspiration capability of the device was tested and analysed under an optical microscope using an aqueous solution of fluorescently labelled nanobeads. The nanopipetting experiments represent an extension over the authors' earlier work which concentrated on the dispensing and imaging capabilities of a similar system.

1. Introduction: Having the means to control, dispense and handle small amounts of liquids is becoming a crucial competence for manipulations at the nanoscale. This has pushed scientists to look for tools that could be useful for performing different kinds of fluidic assays at the nanoscale. An instrument particularly suitable for manipulating matter at such a scale is the atomic force microscope (AFM). The AFM offers the capability of acting not only as a microscope with atomic resolution [1, 2] but also as a nanotool to manipulate molecules [3, 4], displace atoms [5] and reshape complex molecules [6]. As a consequence, this instrument has attracted extensive attention. Its latest achievements in chemistry [7], biology [8] and other fields [9] suggest that it is necessary to further develop microfluidic tools to reach radical advancements. In ongoing efforts to fulfil these needs, different cantilever-based microfluidic devices have been reported [7, 8, 10–13]. The intention has been to mimic the functionality of a standard macroscopic pipette. However, and to our best knowledge, all but two of the reported devices have so far been focusing only on the dispensing aspect of the device. The exceptions used a cantilever without a tip but a larger hole instead to which an entire cell was aspirated [14].

In this Letter, we introduce a method to aspirate liquids through a tip into a hollow cantilever-based nanopipette. The core of the nanopipette consisted of a SiO_2 cantilever that connected an on-chip fluidic reservoir to an Si_3N_4 tip and an evaporation cell. This created a continuous and closed fluidic system that could be filled with an arbitrary chosen liquid. A hole in the tip allowed liquids to be dispensed or aspirated. If mounted on an AFM, optical readout of the cantilever deflection could be used to control force interaction between the tip and the substrate.

We previously reported the fabrication process of the nanopipette [15]. In short, two silicon wafers, one containing the fluidic reservoir and the other one defining the cantilever structure, are potassium hydroxide (KOH) and DRIE etched, respectively. Once patterned, they were aligned and fuse bonded in an oxidising atmosphere, then etched in KOH to release the SiO_2 cantilever. A focused ion beam was used to mill a nozzle next to the apex of the Si_3N_4 tip for dispensing and aspirating. The nozzle had a diameter of 350 nm in this case. The results shown here represent an improvement over our earlier work of dispensing and imaging capabilities only [16].

2. Experiments and discussion: To trigger the aspiration modality, it was necessary to adjust the design of the chip. Instead of having the fluidic cantilever connected to a single fluidic reservoir, a second reservoir, called the evaporation cell, was included. The evaporation cell, featured a larger surface area and an open capillary structure. The U-shaped cantilever was connected to the fluidic reservoir at one end and the evaporation cell at the other end (Fig. 1). Our group has earlier demonstrated a pumping mechanism that generated a continuous flow from the reservoir cavity towards the evaporation cell until the entire liquid had evaporated [17]. Here, we demonstrate that the same pumping mechanism can be used also for aspirating.

The fundamental resonance frequency of the cantilever when it is empty or filled with water is shown in Fig. 2. Frequency was sweeped near the resonance frequency to collect this data. The 155 µm-long cantilever was found to have a resonance frequency of 153.946 kHz when empty. When filled with water, the frequency dropped to 153.854 kHz. Such a shift of 92 Hz happened because of additional mass loading. When the water evaporated, the frequency went back to its original value. This corresponds to a distributed mass change of 2.7 pg.

When a droplet of water was placed in the reservoir, it immediately filled the hydrophilic microfluidic channels of the cantilever because of the capillary effect. Once the liquid reached the evaporation cell, the fluid started evaporating. The capillary effect kept drawing the liquid from the reservoir towards the evaporation cell maintaining the hollow cantilever filled with liquid with a continuous flow until all the liquid evaporated. The advancement of the terminal meniscus as a function of time could be observed because of the transparent cantilever and is shown in Fig. 3.

To increase the flow rate either the evaporation rate could be increased by increasing the area of the evaporation cell or reducing the humidity in the gas phase above it. This not only enhanced the flow rate but also the flow induced pressure drop over the hydraulic resistance of the fluidic system. Consequently, there are two different flow regimes [17]: a low and a high (see Fig. 4). In the high-flow regime, a maximum evaporation induced flow rate was achieved when the pressure drop P_{sys} over the fluidic system equalled the capillary pressure P_{cap}. When this happened, the hydraulic resistance R_{hyd} of the fluidic system and the capillary pressure P_{cap} limited the

doi: 10.1049/mnl.2013.0362

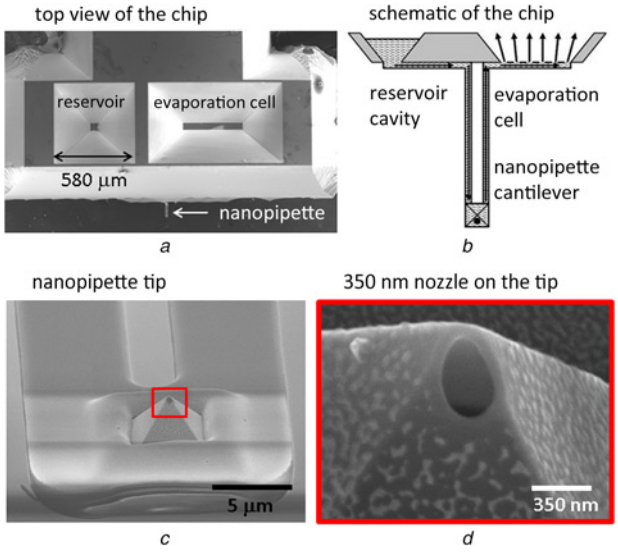

Figure 1 *Top view of chip with fluidic reservoir and evaporation cell connected to either end of U-shaped hollow cantilever nanopipette (fluidic elements located on bottom side of chip (Fig. 1a). Schematic of device (Fig. 1b). SEM image of Si_3N_4 tip connected to SiO_2 hollow cantilever (Fig. 1c) with 350 nm wide nozzle near tip (Fig. 1d). Nozzle near cantilever tip was used for dispensing and aspirating liquids*

flow rate Q. Therefore the capillary pressure P_{cap} could not keep the full surface area of the evaporation cell wetted, and thus, not reach the open channels which were kept wet, reducing Q. Hence, the evaporation rate was self-limited by reducing the evaporation area. In the low-flow regime, the pressure drop over the fluidic system P_{sys} was lower than the capillary pressure P_{cap}, hence the entire surface area of the evaporation cell was kept wet and the flow rate Q was limited by the evaporation rate. During aspiration the chip operated in a low-flow regime, where the capillary pressure P_{cap} dominated the pressure drop P_{sys}.

Each leg of the nanopipette had a fluidic channel with a height of 2.2 µm and a width of 3.7 µm. Owing to these small dimensions, the Reynolds number was 7.26×10^{-6}. This resulted in a completely laminar flow. In addition, the flow was dominated by the interaction between the fluid and the walls of the microchannel rather than by bulk effect [18].

The contact angle (θ) determines the hydrophilicity of a surface [19] and the capillary force on the fluid in the microchannel which has a rectangular cross-section can be calculated using

$$F = 2(w + h)\sigma \cos\theta \tag{1}$$

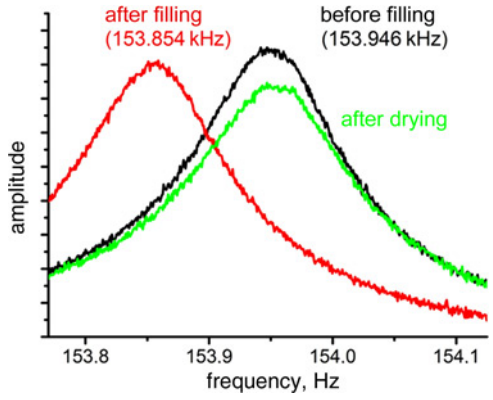

Figure 2 *Shift in resonance frequency obtained when hollow cantilever filled with deionised water and emptied*

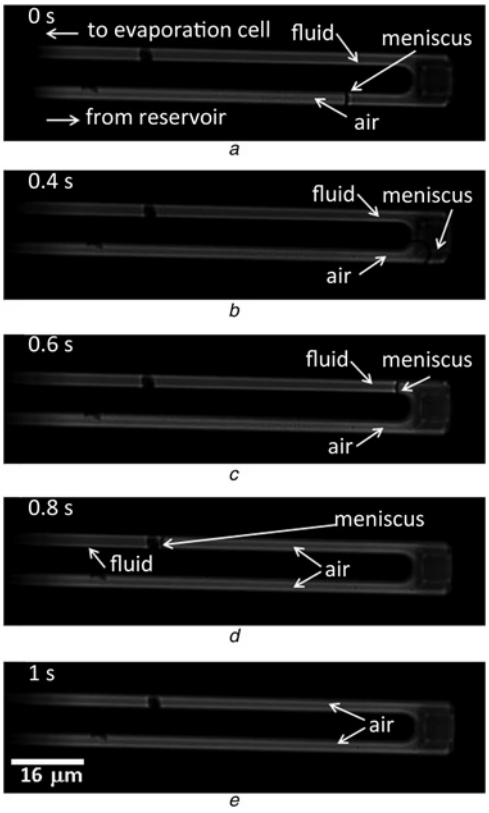

Figure 3 *Motion of terminal meniscus inside cantilever at various instances in time (Figs. 3a–e)*

where w and h are the geometrical size in width and height of the channel, σ is the interfacial tension between air and liquid (σ = 0.0728 J/m^2 for water at room temperature) and θ is the contact angle of the liquid on the channel surface. This force can be represented as an equivalent capillary pressure (P_{cap}) [20]

$$P_{cap} = \frac{F}{A} = \frac{2(w + h)\sigma \cos\theta}{wh} = 2\sigma \cos\theta\left(\frac{1}{w} + \frac{1}{h}\right) \tag{2}$$

Moreover, according to Hagen-Poiseuille's law, the fluidic resistance depends on three factors: the cross-sectional area of the channel, the length of the cantilever and the viscosity of the fluid [21]. The volume flow rate Q, which represents the volume passing through the rectangular channel per time unit could be found by integrating the velocity profile over the cross-sectional

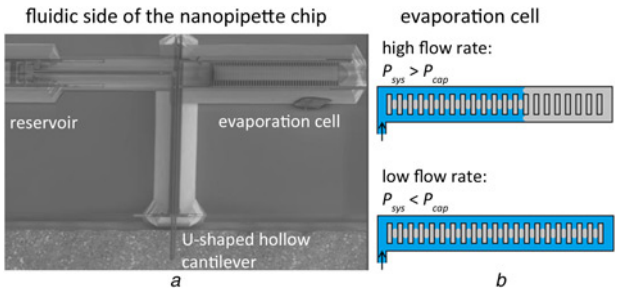

Figure 4 *SEM image of bottom side of nanopipette chip (evaporating water induces continuous fluidic motion from reservoir towards evaporation cell) (Fig. 4a). Different filling levels within evaporation cell depend on flow induced pressure drop over fluidic system P_{sys} and capillary pressure P_{cap} at water–air interface (Fig. 4b)*

area of the channel, resulting in

$$Q = \frac{h^3 w \Delta p}{12 \eta L}\left(1 - 0.63\frac{h}{w}\right) \quad (3)$$

where Δp represents the pressure difference, η represents the viscosity of the liquid and L is the length of the cantilever. According to Poiseuille's law, there is a linear relation between the pressure difference over a channel and the flow

$$\Delta p = R_{\text{hyd}} Q \quad (4)$$

The proportionality factor R_{hyd} known as the hydraulic resistance of a rectangular capillary with $w > h$, [22], is defined as

$$R_{\text{hyd}} = \frac{\Delta p}{Q} = \frac{12 \eta L}{h^3 (w - 0.63\ h)} \quad (5)$$

The total length of the capillary between the reservoir and the evaporation cell was 2.1 mm. This resulted in a hydraulic resistance $R\text{hyd} = 9.12 \times 10^{17}$ Pa-s/m^3. Within the channel, the capillary pressure was calculated to be $P_{\text{cap}} = 0.99$bar. A flow rate of 3.39 fL/s was measured. This value can be interpreted as the volumetric flow rate in the hollow cantilever because of evaporation in the ambient conditions (21°C temperature, 43% relative humidity).

To prove the aspiration, we have conducted experiments for three different cases:

(a) In the first case, an empty cantilever tip was dipped into a solution containing 50 nm fluorescent beads. In such a scenario, no aspiration was observed. Without any liquid inside the hollow cantilever, the pumping mechanism was absent. The hydrodynamic resistance because of small nozzle size was so high that even aspiration because of capillarity was also not observed.

(b) In the second case, a filled cantilever tip having a continuous fluidic motion from the reservoir to the evaporation cell, was dipped into the fluorescent bead solution. No aspiration was observed even in this case. This is attributed to the lower resistance to the fluid coming from the reservoir in comparison to the fluid trying to pass through the nozzle at the tip.

(c) In the third case, again the continuous pumping mechanism was activated, but the last advancing meniscus was used. During the pumping process, the tip was dipped in the fluorescent solution as shown in Fig. 5*a*. At the final stage before the liquid completely evaporated, the advancing meniscus created a negative pressure, as shown in Fig. 5*b*. The moment when the last advancing meniscus passed through the tip zone as previously depicted in Figs. 3*b* and *c*, resulted in the aspiration being triggered. This was strong enough to overcome the resistance because of the nozzle, estimated to be 7.81 bar when dry. As a result, the nanobead solution started getting aspirated while following the last advancing meniscus. This is shown in Fig. 5*c*. This evaporation-induced aspiration is a self-limiting process. Once the terminal water meniscus arrived to the evaporation cell the entire evaporation process stopped. This resulted in an aspirated solution occupying one of the legs of the nanopipette and the surface area of the evaporation cell. The effect is seen in Fig. 5*d*.

Therefore wetting of the nozzle and the final meniscus were necessary for evaporation induced aspiration. The fluorescence image of a cantilever with and without fluorescent nanobeads is shown in Fig. 6. The nanobeads were aspirated into the channel connected to the evaporation cell indicating negative pressure created in that channel. Such negative pressure, together with the cohesion

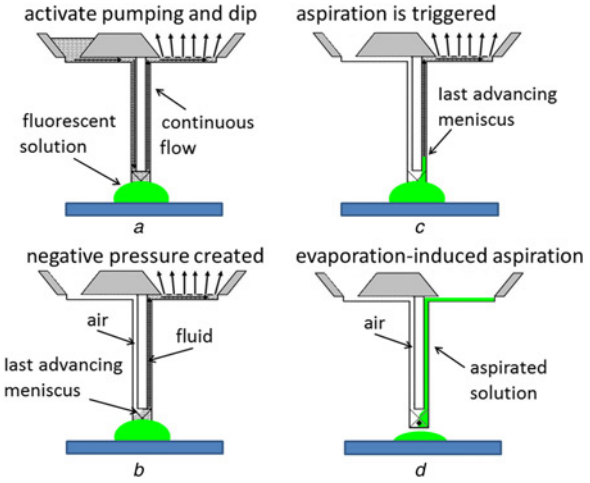

Figure 5 *Evaporation-based pumping had to be activated before aspiration could take place*
Once pumping was active: tip of cantilever dipped into solution containing nanobeads (Fig. 5*a*); once last advancing meniscus of evaporating liquid passed through tip-zone, negative pressure was created (Fig. 5*b*); this negative pressure started aspiration process, which pulled in the fluorescent solution (Fig. 5*c*) until; entire evaporation-induced aspiration self-terminated (Fig. 5*d*)

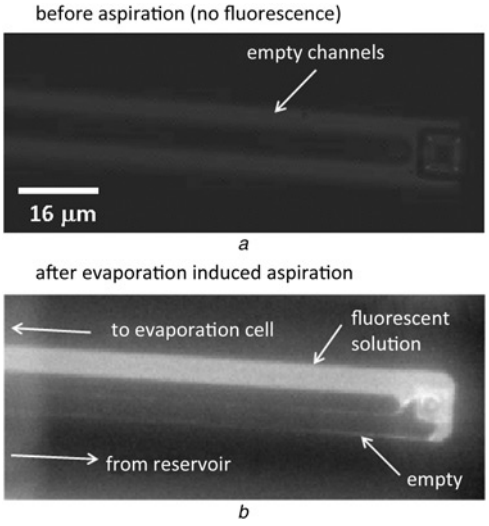

Figure 6 *Fluorescence image of an empty (Fig. 6a) and fluorescent nanobead filled hollow cantilever (Fig. 6b)*
Nanobeads were aspirated into channel where negative pressure was created

Table 1 Summary of characterisation of cantilever-based nanopipette

Parameter	Units
cantilever dimensions (each leg)	L:155 µm, W:6.4 µm, T:4.9 µm
fluidic channel dimensions (each leg)	L:153.5 µm, W:3.7 µm, T: 2.2 µm
nozzle diameter	350 nm
spring constant	3.47 N/m (when empty)
resonance frequency	153.94 kHz (when empty)
quality factor	435
Reynolds number	7.26×10^{-6}
capillary pressure P_{cap}	− 0.99 bar
hydraulic resistance R_{hyd}	9.12×10^{17} Pa-s/m^3
mean velocity of fluidic motion because of evaporation	417.3 µm/s
evaporation induced flow rate Q	3.39 fL/s
pressure to overcome dry nozzle	7.81 bar
aspiration rate	− 230 aL/s
aspirated volume	− 85.42 aL

doi: 10.1049/mnl.2013.0362

between the liquids from across the nozzle, could pull in the fluorescently labelled liquid.

3. Summary and conclusions: To conclude, we have developed an evaporation-based aspiration method suitable for nanopipetting using an AFM chip with a hollow cantilever. We have estimated an aspiration rate and volume of −230 aL/s and −85.42 aL. We have successfully aspirated nanobeads through a 350 nm diameter nozzle using this technique. The complete characteristics of the device and its performance are summarised in Table 1. The aspiration capability makes the nanopipette an ideal tool for cell surgery and for trafficking molecules across the cell wall and between cells.

4. Acknowledgments: This project was in part financed by the NanoNextNL programme and consortium, funded by the Dutch government. The authors acknowledge the members of the Micro and Nano Engineering group for valuable suggestions and fruitful discussions. The authors also thank the members of the technical staff of the DIMES Technology Center at TU Delft for the support provided during fabrication of the devices and their quality control.

5 References

[1] Giessibl F.J.: 'Atomic-resolution of the silicon (111)-(7 × 7) surface by atomic-force microscopy', *Science*, 1995, **267**, (5194), pp. 68–71
[2] Barth C., Reichling M.: 'Imaging the atomic arrangements on the high-temperature reconstructed alpha-Al_2O_3(0001) surface', *Nature*, 2001, **414**, (6859), pp. 54–57
[3] Morita S., Yi I., Sugimoto Y., *ET AL.*: 'Mechanical distinction and manipulation of atoms based on noncontact atomic force microscopy', *Appl. Surf. Sci.*, 2005, **241**, (1–2), pp. 2–8
[4] Oyabu N., Sugimoto Y., Abe M., *ET AL.*: 'Lateral manipulation of single atoms at semiconductor surfaces using atomic force microscopy', *Nanotechnology*, 2005, **16**, (3), pp. S112–S117
[5] Sugimoto Y., Abe M., Hirayamo S., *ET AL.*: 'Atom inlays performed at room temperature using atomic force microscopy', *Nature Mater.*, 2005, **4**, (2), pp. 156–U36
[6] Thalhammer S., Stark R.W., Muller S., *ET AL.*: 'The atomic force microscope as a new microdissecting tool for the generation of genetic probes', *J. Struct. Biol.*, 1997, **119**, (2), pp. 232–237
[7] Rodolfa K.T., Bruckbauer A., Zhou D., *ET AL.*: 'Nanoscale pipetting for controlled chemistry in small arrayed water droplets using a double-barrel pipet', *Nano Lett.*, 2006, **6**, (2), pp. 252–257
[8] Meister A., Gabi M., Behr P., *ET AL.*: 'FluidFM: combining atomic force microscopy and nanofluidics in a universal liquid delivery system for single cell applications and beyond', *Nano Lett.*, 2009, **9**, (6), pp. 2501–2507
[9] Kley V.B.: US patent 6,354,219 B1, 2002
[10] Kim K.H., Moldovan N., Ke C., *ET AL.*: 'A novel AFM chip for fountain pen nanolithography – design and microfabrication', *Micro Nanosyst.*, 2004, **782**, pp. 267–272
[11] Piner R.D., Zhu J., Xu F., *ET AL.*: '"Dip-pen" nanolithography', *Science*, 1999, **283**, (5402), pp. 661–663
[12] Meister A., Jeney S., Liley M., *ET AL.*: 'Nanoscale dispensing of liquids through cantilevered probes', *Microelectron. Eng.*, 2003, **67–8**, pp. 644–650
[13] Leichle T., Lishchynska M., Mathieu F., *ET AL.*: 'A microcantilever-based picoliter droplet dispenser with integrated force sensors and electroassisted deposition means', *J. Microelectromech. Syst.*, 2008, **17**, (5), pp. 1239–1253
[14] Dorig P., Stiefec P., Behr P., *ET AL.*: 'Force-controlled spatial manipulation of viable mammalian cells and micro-organisms by means of FluidFM technology', *Appl. Phys. Lett.*, 2010, **97**, (2), p. 023701
[15] Hug T.S., Biss T., de Rooij N. F., *ET AL.*: 'Generic fabriction technology for transparent and suspended microfluidic and nanofluidic channels'. Transducers '05, Dig. Tech. Pprs, 2005, vol. 1 and 2, pp. 1191–1194
[16] Perez Garza H.H., Ghatkesar M., Staufer U.: 'Combined AFM-nanopipette cartridge system for actively dispensing femtolitre droplets', *J. Micro-Bio Robot.*, 2013, **8**, (1), pp. 33–40
[17] Heuck F., Hug T., Akiyama T., *ET AL.*: 'Evaporation based micro pump integrated into a scanning force microscope probe', *Microelectron. Eng.*, 2008, **85**, (5–6), pp. 1302–1305
[18] Kumar C.S.S.R.: 'Microfluidic devices in nanotechnology: applications' (John Wiley & Sons, Hoboken, New Jersey, 2010)
[19] Chesworth W.: 'Encyclopedia of soil science' (Springer, Dordrecht, The Netherlands, 2008), p. 902
[20] Zhang R.J., Ikoma Y., Motooka T.: 'Negative capillary-pressure-induced cavitation probability in nanochannels', *Nanotechnology*, 2010, **21**, (10), p. 105706
[21] CORD Communications: 'Physics in context: an integrated approach' (CCI Publishing, 2001)
[22] Heuck F.: 'Developing and analysing sub-10 μm fluidic systems with integrated electrodes for pumping and sensing in nanotechnology applications'. PhD Thesis, 2010